Thermomechanical properties of interpenetrating graphite/aluminium composites produced by the indirect squeeze casting process

T. Etter[1], J. Kuebler[2], T. Frey[1], P. Schulz[3], P. J. Uggowitzer[1]

[1]Laboratory of Metal Physics and Technology, Departement of Materials, ETH Zürich, Sonneggstrasse 3, CH-8092 Zürich, Switzerland
[2]EMPA, Swiss Federal Laboratories for Materials Testing and Research, Überlandstrasse 129, CH-8600 Dübendorf, Switzerland
[3]ARC Leichtmetallkompetenzzentrum Ranshofen GmbH, Amag – FVA- Gebäude, Postfach 26, A-5282 Ranshofen, Austria

ABSTRACT

Interpenetrating graphite/aluminium composites were produced by the indirect squeeze casting process. Isotropic graphite preforms, with an open porosity of about 14.5 vol%, were infiltrated using either an AlSi7Ba or an AlSi12 alloy. Flexural strength and fracture toughness were determined at room temperature and 300°C before and after thermal cycling. The infiltration with AlSi7Ba alloy increases the flexural strength of the composites, resulting in values up to 120 MPa at room temperature. At the same time, the toughening metal phase enhances the fracture toughness from 0.94 $MPam^{1/2}$ for the porous preform to 1.93 $MPam^{1/2}$ for corresponding composites. Weibull moduli m of the graphite preform and composites are higher than 20. The metal infiltration does not enhance the Weibull modulus in C/Al composites compared to the porous preform. At 300°C no decrease in flexural strength and fracture toughness is observed. After thermal cycling, a slight reduction of the mechanical properties for graphite/AlSi7Ba composites is observed, mainly due to precipitation reactions and silicon phase coarsening during thermal cycling. The contribution of the ductile metal phase to enhanced fracture toughness in composites is explained by an analytical consideration of a crack bridging model.

1. INTRODUCTION

Compared to monolithic materials, improved mechanical and physical properties may be obtained by producing interpenetrating phase composites. These composites can be defined as multiphase materials in which each phase is three-dimensionally interconnected throughout the microstructure, allowing multifunctional characteristics [1]. Such attractive combination of properties is not possible if one of the phases is isolated as particles or fibres.

In this work graphite/aluminium (C/Al) composites with an interpenetrating network microstructure have been produced by means of indirect squeeze casting process. The principle of the infiltration of porous graphites with light metals is to force the liquid melt into the preform under external pressure to overcome the bad wettability between aluminium and graphite. Due to their specific properties, light metal infiltrated graphites may be attractive for lightweight components such as parts of internal combustion engines or current collectors [2]. As for application as piston material, the low coefficient of thermal expansion and the temperature resistance of carbon materials in addition to the low density enable a significant fuel and oil reduction compared to pistons made of conventional monolithic alloys. In order to fulfil the mechanical requirements of the automotive industry for piston materials, a metal reinforcement of porous graphite turns out to be a necessity.

For different ceramic/metal composite systems the incorporation of a ductile metal phase is known to improve mechanical properties compared to monolithic ceramic preforms. For example, Al_2O_3/Al composites manufactured by gas pressure metal infiltration exhibit strength levels of up to 710 MPa and toughness levels of 5.4 $MPam^{1/2}$, compared to 150 MPa and 1.9 $MPam^{1/2}$ for the porous alumina preform (25 vol% porosity) [3]. The main strengthening/toughening mechanism assumed to be effective in reinforced ceramics is the plastic stretching of the ductile metallic phase [3, 4]. This bridging mechanism can be even more effective in conjunction with residual compressive stresses in the ceramic phase, induced by thermal expansion mismatch between the ceramic and the metal phase [5].

In this paper the indirect squeeze casting method was used to fabricate C/Al composites. Flexural strength and fracture toughness of porous graphite preforms as well as of composites

infiltrated with AlSi7Ba or AlSi12 were measured at room temperature and at 300°C, respectively. These properties were determined for samples in the as produced condition and after thermal cycling (TC) treatment.

2. EXPERIMENTAL

2.1 Monolithic materials

An isotropic polycrystalline porous graphite with an open porosity of about 14.5 vol%, manufactured by Schunk Kohlenstofftechnik GmbH (Germany), was used as a preform. The graphite preforms were infiltrated either with AlSi7Ba (7 wt% Si, 0.25 wt% Ba) or eutectic AlSi12 (12 wt% Si) alloy.

The addition of surface active elements like barium to an AlSi7 base alloy should facilitate the infiltration [6] by lowering the surface tension of the liquid aluminium alloy. A slightly increased metal content and modified interface bonding compared to C/AlSi12 is expected.

2.2 Indirect squeeze casting process

All graphite preforms with dimension 150x65x22 mm^3 were infiltrated with a UBE HVSC 350 indirect squeeze casting machine at ARC in Ranshofen, Austria. The superheated aluminium melts (750°C) were pressed into preheated graphite preforms (680°C) with a hydraulic plunger and solidified under a pressure of about 75 MPa. An infiltration cycle required about 60 s.

2.3 Microstructural characterisation and mechanical testing

Microstructural characterisation was obtained with a Polyvar MET microscope (Reichert Jung) equipped with a Leica DC 200 camera, after chemical etching with Keller's reagent. Scanning electron microscopy (SEM) was carried out with a Cam-Scan CS4 scanning electron microscope operating at a voltage of 20 kV.

In order to determine the flexural strength, four-point bending tests at room temperature were performed on an Instron 8562 universal testing machine using a crosshead speed of 1 mm/min. All bending test samples were 3x4x45 mm^3 in size. Four-Point flexural strength at 300°C was measured on a Zwick 1478 machine. The heating rate for all samples was 15°C/min. Before testing, the temperature was held constant at 300°C for 15 min.

Fracture toughness tests at room temperature with porous graphite preforms and infiltrated composites were performed by means of the SEVNB method (single edge V-notched beam) [7], using five bars of each material of the same size as used for the flexural strength tests. With this method, we could achieve notch tip radii of about 30 μm. The measurements were performed with a Zwick 1478 using a crosshead speed of 1 mm/min.

To investigate the susceptibility of this composite to thermal fatigue, the specimens were thermally cycled between room temperature and 300°C with a modified Heraeus furnace. The thermal cycling was performed 1000 times using the pneumatic motion of a hollow sample holder. The samples were cooled to room temperature by cold air of a hair blower, achieving a cooling rate of 5°C/s.

3. RESULTS AND DISCUSSION

3.1 Material characterisation

A typical microstructure of C/AlSi7Ba composites is shown in Fig. 1. The metal phase (bright) filled the pores homogeneously. For both composites, C/AlSi7Ba and C/AlSi12, the residual open porosity determined by mercury porosimetry was less than 1 vol%. At higher magnifications, as shown in Fig. 2, the silicon phase in the metal matrix became visible after etching the composites for 5 s in Keller's reagent.

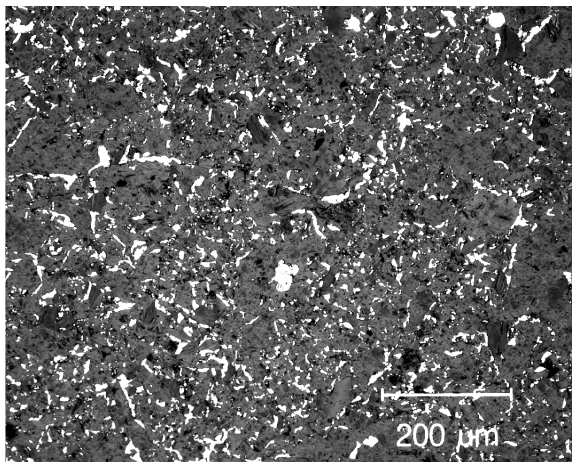

Fig. 1. Optical micrograph of C/AlSi7Ba composite.

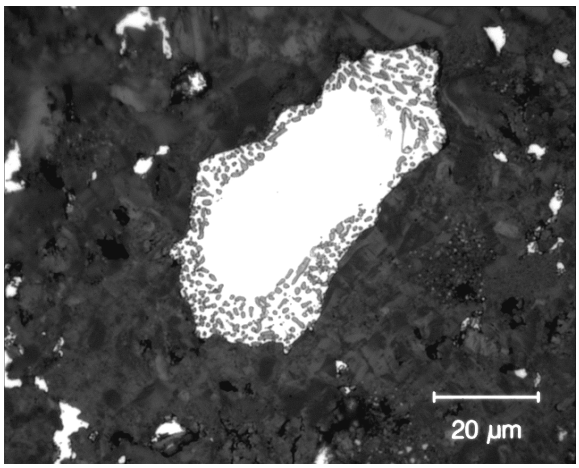

Fig. 2. Si distribution in C/AlSi7Ba composite before thermal cycling (TC).

The microstructure of the metal phase in C/AlSi7Ba composites is characterized by the formation of about 50 vol% primary α-aluminium and 50 vol% eutectic. The α-aluminium is assumed to nucleate at the C/melt interface. At the eutectic temperature half of the pore volume is filled with α-aluminium, with the residual melt located between α-aluminium and graphite. Consequently, in C/AlSi7Ba the silicon phase is predominantly arranged along the C/metal interface (Fig. 2).

3.2 Mechanical properties

3.2.1 Flexural strength

Flexural strength properties of the graphite preform and the corresponding C/AlSi7Ba and C/AlSi12 composites measured at room temperature and 300°C before thermal cycling are shown in Fig. 3. The values for C/AlSi7Ba and C/AlSi12 measured at room temperature represent the average of 6 and 15 specimens, respectively.

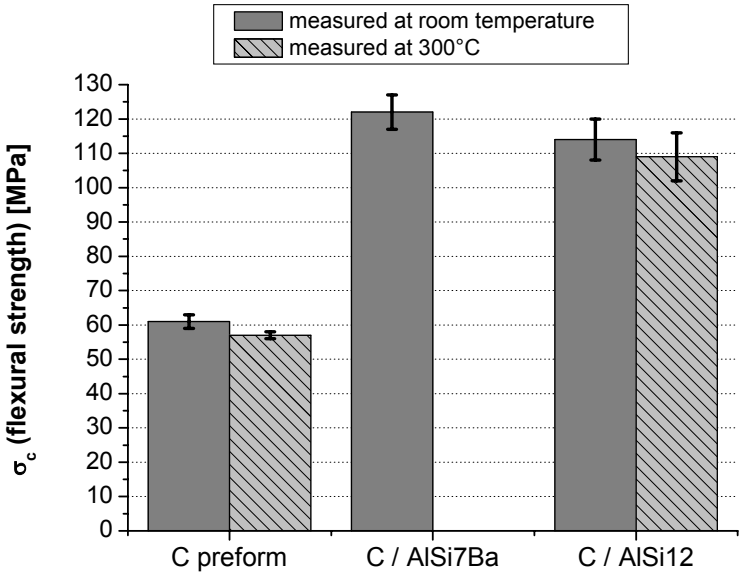

Fig. 3. Flexural strength of porous graphite and corresponding composites at room temperature (RT) and 300°C.

The flexural strength of the composites increases by a factor of two, compared to the respective porous graphite preform. This increase of about 60 MPa cannot be explained by a strength contribution of the aluminium phase calculated from a simple rule of mixture. As

discussed in the following chapter, it is more appropriate to relate the strength increase to the enhanced toughness of the interpenetrating C/Al composites. The values in Fig. 3 indicate that the chemical composition of the metallic matrix has no significant influence on the flexural strength. Within experimental error, the flexural strength values of C/AlSi7Ba and C/AlSi12 are of similar level.

Five samples of porous graphite and C/AlSi12, respectively, were tested to measure the flexural strength at 300°C. Although graphite materials show an increase in strength by heating up to 2500° or even 2600°C [8], this desirable property could not be observed at 300°C, as can be seen in Fig. 3. However, although the mechanical strength of the aluminium alloy at 300°C is only a fraction of the room temperature strength, the composite shows no decrease in strength at elevated temperature. Again, the increase in strength of the composite cannot simply be explained by only considering the strength of the metal phase as is done in the rule of mixtures. It does rather reflect the enhanced fracture toughness of interpenetrating composites.

The characteristic Weibull statistics for porous graphite and C/AlSi12 composites are illustrated in Fig. 4.

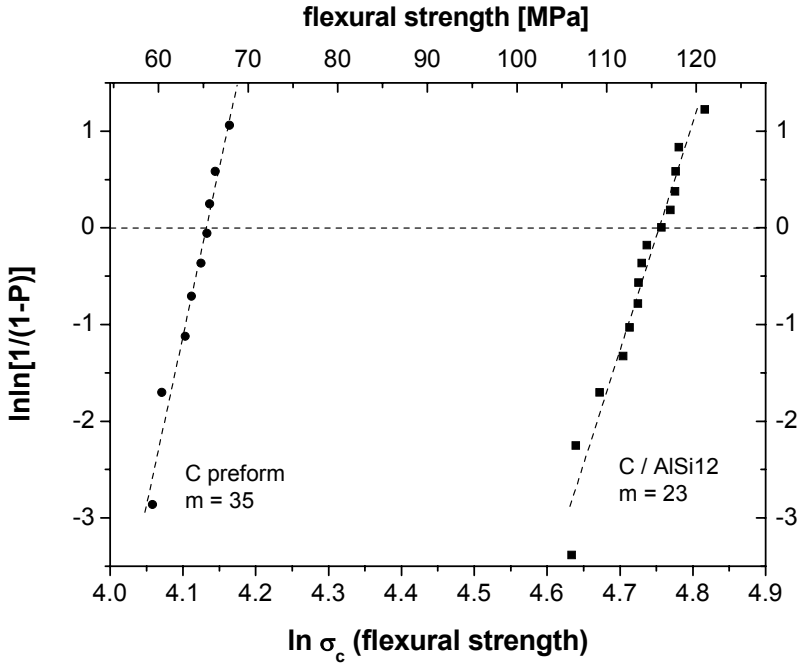

Fig. 4. Weibull distribution for the porous C preform and the corresponding C/AlSi12 composites.

As can be seen in Fig. 4, the aluminium infiltration did not enhance the Weibull modulus. The difference in Weibull moduli for the graphite preform (m=35) and the C/AlSi12 composites (m=23) can be attributed to the different number of measured samples.

3.2.2 Fracture toughness

The material's deformation behaviour can be considered as indicator for failure tolerance capability. For the monolithic graphite preform, as a brittle ceramic material, a linear behaviour according to Hooke's law is expected and was observed experimentally. The infiltration of the metal phase, however, results in a deviation from linearity which indicates a partly ductile and, therefore, more failure tolerant behaviour of the composite. Fig. 5 shows the fracture toughness of graphite preforms and the corresponding composites determined at room temperature and 300°C before TC treatment.

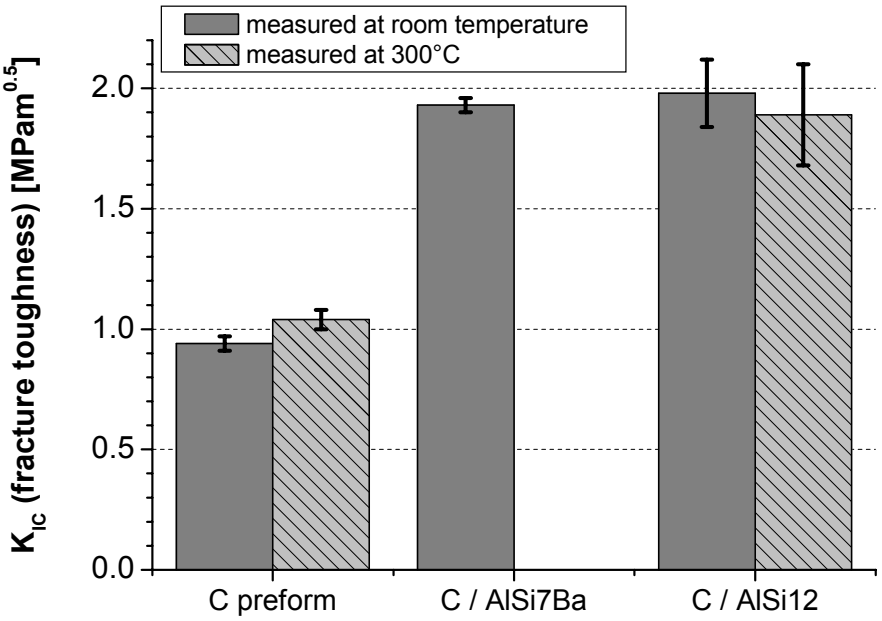

Fig. 5. Fracture toughness of porous C preform and corresponding composites at room temperature and 300°C determined before thermal cycling.

Similar to the flexural strength, the infiltration of the ductile metal phase has doubled the fracture toughness. It increased from 0.94 MPam$^{1/2}$ for porous graphite to 1.93-1.98 MPam$^{1/2}$ for metal-infiltrated composites. This toughness values are significantly higher than the fracture toughness levels reported for different graphite structures. For example, for nuclear graphites fracture toughness levels were measured within the range of 0.75 MPam$^{1/2}$ to 1.5 MPam$^{1/2}$ [8]. In [9] a fracture toughness of 1.12 MPam$^{1/2}$ is published for graphite with a porosity of 15 vol%.

SEM analysis of fracture surfaces in C/Al composites revealed mixed fracture behaviour. Cleavage fracture of graphite grains along the basal plane, crack propagation between grains and along the C/metal interface as well as plastically deformed aluminium was observed. Due to the fact that aluminium is much more ductile than graphite, the metal phase provides a significant resistance to crack propagation in composites. The interconnected morphology forces the advancing crack to pass through the metal phase, thereby enhancing the toughness by energy absorption of the plastically deforming aluminium. Fig. 6 and Fig. 7 show the fracture surface of C/AlSi7Ba and C/AlSi12 composites, respectively.

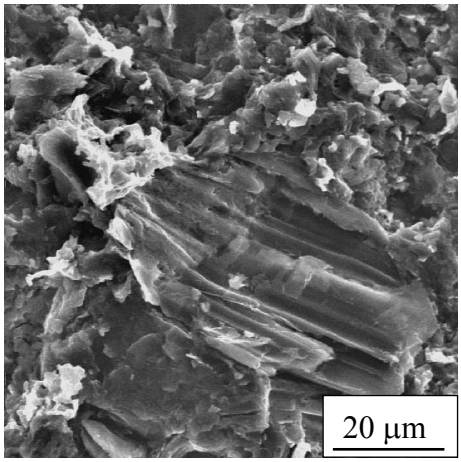

Fig. 6. SEM fracture surface of C/AlSi7Ba composite.

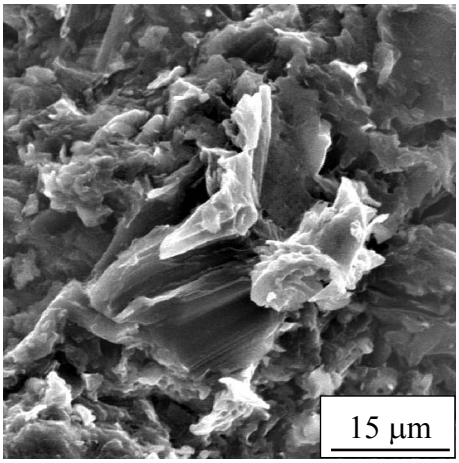

Fig. 7. SEM fracture surface of C/AlSi12 composite.

The contribution of ductile material bridging to the fracture toughness of interpenetrating phase composites was estimated by Wegner and Gibson [10]. According to their model, an increase in fracture toughness ΔK_{Jb} by ductile metal reinforcement can be formulated as

$$\Delta K_{Jb} = \sqrt{\Delta J_b E} = \sqrt{\frac{2 f_b^2 d_{Gr} \sigma_Y \varepsilon^*}{3(1-f_b)} E} \tag{1}$$

where f_b is the volume fraction of the bridging phase (aluminium alloy), σ_y is the mean of the yield and ultimate tensile strength of the bridging phase, ε^* is the failure strain, d_{Gr} is the mean distance of the bridging aluminium phase and E is the Young's modulus of the composite. According to [3] the fracture toughness in composites K_c is composed of a crack tip toughness term and a microstructural term, which sums up all the active closure stresses of the reinforcement. The crack tip toughness of the C/Al composites is assumed to be equal to the fracture toughness of the corresponding porous graphite preform ΔK_{Gr}. Under these assumptions, we estimate a composite toughness of $K_c = \Delta K_{Gr} + \Delta K_{Jb}$: $1.4\,\mathrm{MPam}^{1/2}$. This value is lower than the measured values illustrated in Fig. 5. Deviations may arise from the assumptions made for d_{Gr} and σ_y. Furthermore, the flow strength and fracture strain in constrained plastic material differ from the mechanical properties in unconstrained material [11]. In addition, the fracture toughness may also be influenced by interface properties and residual stresses, which are not considered in Eq. (1). Nevertheless, Eq. (1) seems to be suitable to roughly estimate the increase in toughness by ductile metal reinforcement. Apparently, for a constant metal volume, a larger pore diameter will influence the fracture toughness more effectively than thin metal ligaments.

The observation of similar flexural strength at room temperature and at 300°C in Fig. 3 is the result of similar fracture toughness at both temperatures and can be explained by Eq. (1). Obviously, it is the term $\sigma_y \varepsilon^*$ in Eq. (1) that is of special relevance for the fracture toughness level. Even if σ_y at 300°C is lower than at room temperature the assumption of increased failure strain seems to be reasonable.

For this brittle C/Al composite it is appropriate to consider flexural strength and fracture toughness as mutually dependent properties. According to [12], the flexural strength σ_c can be derived from K_{IC} by:

$$\sigma_c = \frac{K_{IC}}{Y\sqrt{a}} \tag{2}$$

where a is the size of internal defects and Y is a geometric factor. Under the reasonable assumption of identical defect size in both, the graphite preform and the infiltrated composites, the level of the flexural strength reflects the level of the fracture toughness. The insertion of values of about 1.13 ("penny" shaped defect) and 2 (surface defect) for the geometric factor Y in Eq. (2) results in a critical defect size of 190 µm and 60 µm, respectively. In Fig. 8 and Fig. 9, graphite agglomerates or large graphite grains can be identified as such critical internal defects.

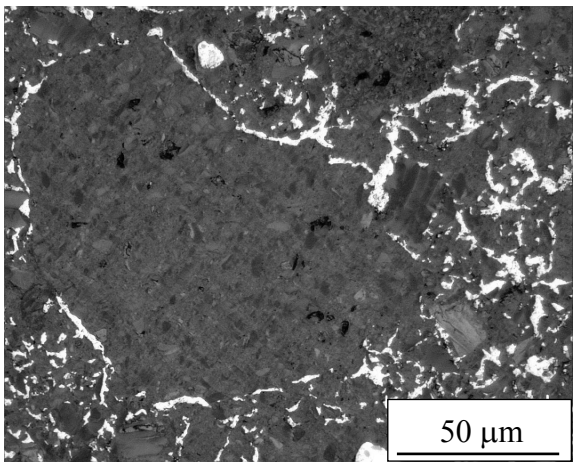

Fig. 8. Optical micrograph of a graphite agglomerate in C/AlSi7Ba composite.

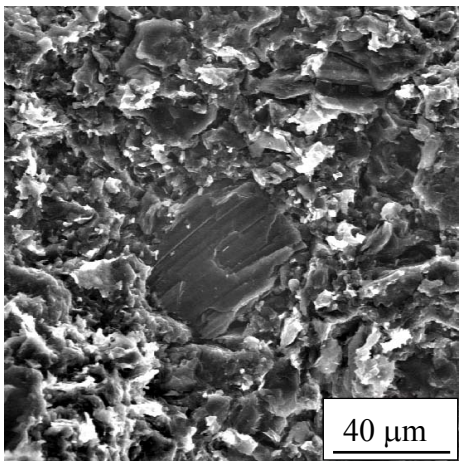

Fig. 9. Fracture surface of C/AlSi12 with coarse graphite grain.

From Table 1 it is clearly visible, that thermal loading affects the fracture toughness of C/AlSi7Ba composites. This effect is less apparent in the C/AlSi12 composites. As expected, the fracture toughness of uninfiltrated graphite is not affected by TC treatment.

Table 1. Fracture toughness (K_{IC}) determined at room temperature (RT) before and after thermal cycling.

	C preform	C / AlSi7Ba	C / AlSi12
K_{IC} before TC [MPam$^{0.5}$]	0.94 ± 0.03	1.93 ± 0.03	1.98 ± 0.14
K_{IC} after TC [MPam$^{0.5}$]	0.93 ± 0.04	1.65 ± 0.02	1.78 ± 0.18

The same tendency is observed for the flexural strength. The C/AlSi7Ba composites show a decrease in flexural strength of about 7 %, whereas C/AlSi12 shows no significant influence of thermal loading. Again, this behaviour can be explained by means of the effect of the microstructure of the metallic phase on the fracture toughness. The decrease of mechanical properties due to TC treatment is apparently caused by a modification of the metal phase. Precipitation of silicon particles and coarsening of the eutectic silicon phase during TC treatment are the most obvious effects. The precipitates are visible after etching as small black points inside the primary aluminium phase of C/AlSi7Ba in Fig. 9.

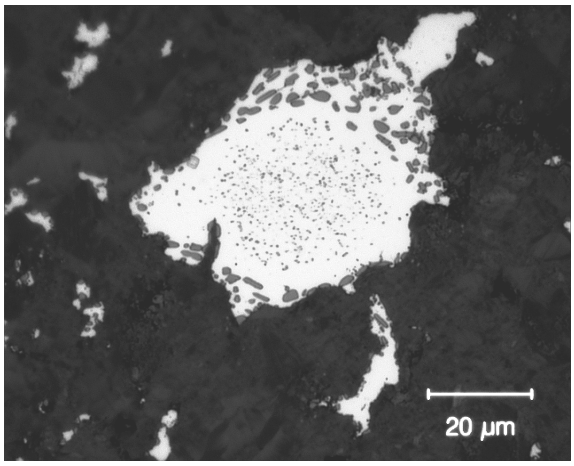

Fig. 9. Silicon precipitation and coarsening in C/AlSi7Ba composite after TC.

Due to the precipitation of silicon in C/AlSi7Ba, a deterioration of the mechanical properties is expected. Thus, the term $\sigma_y \varepsilon^*$ in Eq. (1) decreases, indicating a reduced contribution of the ductile ligament deformation to the fracture toughness of the composites.
Changes in stress distribution during thermal loading are also assumed to contribute to the toughness of the composites. Due to the mismatch of CTE between the graphite and the metal phase, stresses are built up during cooling after infiltration. Since the aluminium phase has a higher CTE than graphite, residual tensile stresses exist in the metal phase and residual compressive stresses occur in the graphite. Neutron diffraction measurements on interpenetrating Al_20_3/Al composites confirmed the assumption about stress distribution mentioned above, keeping in mind that interfacial strength in Al_20_3/Al will be different than in C/Al composites [5]. Therefore residual stresses can affect the toughness, because the residual compressive stresses must first be overcome before a critical load may be applied to a defect [5]. Stress relaxation processes during TC treatment are expected to lower the residual compressive stresses in graphite and therefore lower the critical load for crack formation. Local debonding along the C/Al interface due to the mismatch of CTE between the two constituents is probably an additional reason for the lower fracture toughness after TC treatment.

4. CONCLUSIONS

Interpenetrating phase composites were produced by means of an indirect squeeze casting process. Porous graphite preforms with an open porosity of about 14.5 vol% were infiltrated with AlSi7Ba or an eutectic AlSi12 alloy. Infiltrating the porous preform with aluminium alloys doubles the level of both, the flexural strength and the fracture toughness. The flexural strength and fracture toughness of the composites does not decrease at 300°C. As could be shown by SEM micrographs and theoretical considerations, the significant increase in fracture toughness due to small additions of a ductile metal phase can be attributed to crack bridging by plastic deformation of the metal phase. Thermal cycling experiments pointed out that the mechanical properties can be sensitive to thermal loading depending on the infiltrated metal matrix. The decrease in fracture toughness due to thermal cycling is mainly attributed to aging. However, stress relaxation processes and local debonding may also contribute to this effect.

ACKNOWLEDGEMENTS

The authors would like to thank Schunk Kohlenstofftechnik GmbH for financial support and for delivering the porous graphite preforms, ARC Leichtmetallkompetenzzentrum Ranshofen GmbH for the infiltration work and R. Bächtold from EMPA for support in mechanical measurements. Additionally, the authors would like to express their gratitude to the European Commission for funding parts of this work under Contract No. G3RD-CT-2002-00799.

References

[1] **Clarke, D.R.**, "Interpenetrating phase composites", *J. Am. Ceram. Soc.*, **75**/4 (1992), 739-758.
[2] **Etter, T., Papakyriacou, M., Schulz, P.** and **Uggowitzer, P.J.**, "Physical properties of graphite/aluminium composites produced by gas pressure infiltration method", *Carbon*, **41** (2003), 1017-1024.
[3] **Prielipp, H., Knechtel, M., Claussen, N., Streiffer, S.K., Müllejans, H., Rühle, M.** and **Rödel, J.**, "Strength and fracture toughness of aluminum/alumina composites with interpenetrating networks", *Mater. Sci. Eng. A*, **197** (1995), 19-30.
[4] **Sigl, L.S., Mataga, P.A., Dalgleish, B.J., McMeeking, R.M.** and **Evans, A.G.**, "On the toughness of brittle materials reinforced with a ductile phase", *Acta. Metall.*, **36** (1988), 945-953.
[5] **Hoffmann, H., Roedel, J., Skirl, S., Zimmermann, A., Fuller, E.** and **Mullejans, H.**, "Tailoring of an interpenetrating network ceramic/metal microstructure to improve strength: Al2O3/Ni3Al and Al2O3/Al", *Key. Eng. Mater.*, **159-160** (1999), 311-318.

[6] **Lang, G.**, "Einfluss von Zusatzelementen auf die Oberflächenspannung von flüssigem Reinstaluminium", *Aluminium*, **50** (1974), 731-734.
[7] **Kübler, J.J.**, "Fracture toughness of ceramics using the SEVNB method; From a preliminary study to a standard test method", in: J.A. Salem, G.D. Quinn, and M.G. Jenkins, (Eds.), Fracture resistance testing of monolithic and composite brittle materials, ASTM STP 1409, American society for testing and materials, West Conshohocken, PA, 2002, 93-106.
[8] **Burchell, T.D.**, editor, Carbon materials for advanced technologies, Amsterdam: Pergamon, 1999.
[9] **Salazar, A., Pastor, J.Y.** and **Llorca, J.**, "In situ observation of damage nucleation in graphite and carbon/carbon composites", *Carbon*, **40** (2002), 609-616.
[10] **Wegner, L.D.** and **Gibson, L.J.**, "The fracture toughness behaviour of interpenetrating phase composites", *Int. J. Mech. Sci.*, **43** (2001), 1771-1791.
[11] **Ashby, M.F., Blunt, F.J.** and **Bannister, M.**, "Flow characteristics of highly constrained metal wires", *Acta. Metal.*, **37** (1989), 1847-1857.
[12] **Munz, D.** and **Fett, T.**, Mechanisches Verhalten keramischer Werkstoffe, Springer-Verlag, Berlin, 1989.